

Tensionless contact of a finite beam: Concentrated load inside and outside the contact zone

Yin Zhang · Kevin D. Murphy

Received: 28 February 2013 / Revised: 8 April 2013 / Accepted: 15 May 2013

©The Chinese Society of Theoretical and Applied Mechanics and Springer-Verlag Berlin Heidelberg 2013

Abstract For a finite beam with a nonzero gap distance, an asymmetric concentrated load can be either inside or outside of the contact zone. A new governing equation is given for the case of a concentrated load outside the contact zone. By numerically solving the left-side and right-side contact lengths of the beam, a criterion is established to determine whether the concentrated load is inside or outside the contact zone. A more general approach on the tensionless contact of a beam is thus presented.

Keywords Tensionless contact · Lift-off · Beam

1 Introduction

Tensionless contact, which is variably referred to as unbonded contact, unilateral, or receding contact [1, 2], is to describe the contact of a flexural structure, which may lift-off, or say, separates from its contacting substrate due to the structural flexibility. The contact problem of a flexural structure is encountered in the indentation of such one-dimensional nanostructures as nanobelt [1] and nanowire [2], or in the stiction of microcantilever [3, 4]. An implicit assumption of the previous works on the tensionless contact of a beam or a plate is that the concentrated load is within

the contact zone [1, 2, 5–8]. For a finite [1, 2] or an infinite beam [5, 6] with zero gap distance from its contacting substrate, this assumption is always true. However, for a finite beam with a nonzero gap distance [3, 4, 7], this assumption may not hold. For example, when a nanoindenter indents a micro-cantilever, which is modeled as a concentrated load applied to a beam, the concentrated load is shown to be outside the contact zone [4]. Because of lift-off, only a portion of beam is in contact with the substrate [1, 2, 5–7]. When an asymmetric concentrated load acts on a beam with a nonzero gap distance, the location of the beam maximum displacement is in general different from that of the concentrated load. Physically, the contact zone is the neighborhood around the location of the beam maximum displacement. The concentrated load can thus be outside the contact zone. Two sets of the governing equations are presented for the scenarios of the concentrated load inside and outside the contact zone. A criterion is also given to tell which set of the governing equations should apply.

2 Problem formulation

Figure 1 is a schematic of a finite beam separated from a substrate with a nonzero gap distance of Z_0 . The coordinate system is also shown in Fig. 1. The beam is under a concentrated load of P . E , L and I are the beam Young's modulus, length and the area moment of inertia, respectively. L_1 and L_2 are the distances between P and the left and right ends of the beam. Clearly, $L_1 + L_2 = L$. The beam deflection of W as shown in Fig. 1 is divided into the following three parts

$$W = \begin{cases} W_1, & \text{left-side lift-off region,} \\ W_2, & \text{contact region,} \\ W_3, & \text{right-side lift-off region.} \end{cases} \quad (1)$$

When P is inside the contact zone, the following governing equation set holds [5, 7]

$$EI \frac{d^4 W_1}{dx^4} = 0, \quad W_1 < Z_0, \quad -L_1 < X < X_1,$$

The project was supported by the National Natural Science Foundation of China (110212622 and 11023001) and Chinese Academy of Sciences (KJCX2-EW-L03).

Y. Zhang (✉)

State Key Laboratory of Nonlinear Mechanics,
Institute of Mechanics, Chinese Academy of Sciences,
100190 Beijing, China
e-mail: zhangyin@lnm.imech.ac.cn

K.D. Murphy

Department of Mechanical Engineering,
University of Connecticut,
Storrs, CT 06268, USA

$$EI \frac{d^4 W_2}{dX^4} + k(W_2 - Z_0) = P\delta(X),$$

$$W_2 > Z_0, \quad X_1 < X < X_2, \quad (2)$$

$$EI \frac{d^4 W_3}{dX^4} = 0, \quad W_3 < Z_0, \quad X_2 < X < L_2,$$

where $\delta(X)$ is the Dirac delta function. X_1 and X_2 are the points at which the beam separates from the substrate, as shown in Fig. 1. k is the modulus of the Winkler elastic foundation to model the contacting substrate. For the contact between a beam with Young's modulus of E_1 and a substrate with Young's modulus of E_2 , k is given as follows [9]

$$k = 0.71 E_2 \left(\frac{E_2 B^4}{E_1 I} \right)^{1/3}. \quad (3)$$

Here $2B$ is the beam width.

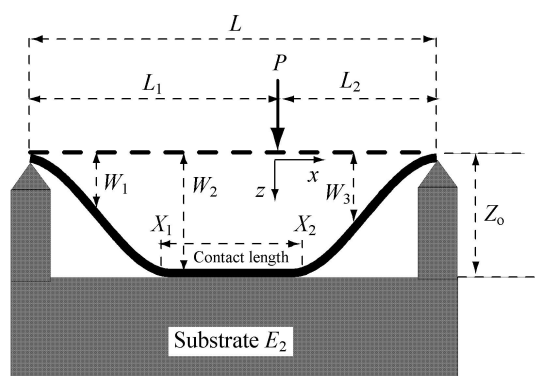


Fig. 1 Schematic diagram of a finite beam with a nonzero gap distance and the coordinate system

When P is outside the contact zone, the following governing equation set holds

$$EI \frac{d^4 W_1}{dX^4} = 0, \quad W_1 < Z_0, \quad -L_1 < X < X_1,$$

$$EI \frac{d^4 W_2}{dX^4} + k(W_2 - Z_0) = 0, \quad W_2 > Z_0, \quad X_1 < X < X_2, \quad (4)$$

$$EI \frac{d^4 W_3}{dX^4} = P\delta(X), \quad W_3 < Z_0, \quad X_2 < X < L_2.$$

Here $L_1 \geq L_2$ is assumed and P thus locates in the right-side lift-off zone of W_3 . If $L_1 \leq L_2$, P will be in the left-side lift-off zone of W_1 . Here only the case of $L_1 \geq L_2$ is computed.

The following nondimensionalization scheme is introduced for computation comparison [5, 7]

$$\xi_1 = \beta X_1, \quad \xi_2 = \beta X_2, \quad l_1 = \beta L_1,$$

$$l_2 = \beta L_2, \quad l = \beta L, \quad z_0 = \beta Z_0, \quad (5)$$

$$w = \beta W, \quad \xi = \beta X, \quad F = \frac{P}{4\beta^2 EI},$$

where β is a parameter defined as follows

$$\beta^4 = \frac{k}{4E_1 I}, \quad (6)$$

with the unit of m^{-1} . Physically, β^{-1} is also the length used to evaluate the effect of beam bending on the contact [10].

Equation (2) is now nondimensionalized as

$$\frac{d^4 w_1}{d\xi^4} = 0, \quad w_1 < z_0, \quad -l_1 < \xi < \xi_1,$$

$$\frac{d^4 w_2}{4d\xi^4} + w_2 - z_0 = F\delta(\xi), \quad w_2 > z_0, \quad \xi_1 < \xi < \xi_2, \quad (7)$$

$$\frac{d^4 w_3}{d\xi^4} = 0, \quad w_3 < z_0, \quad \xi_2 < \xi < l_2.$$

Equation (4) is now nondimensionalized as

$$\frac{d^4 w_1}{d\xi^4} = 0, \quad w_1 < z_0, \quad -l_1 < \xi < \xi_1,$$

$$\frac{d^4 w_2}{4d\xi^4} + w_2 - z_0 = 0, \quad w_2 > z_0, \quad \xi_1 < \xi < \xi_2, \quad (8)$$

$$\frac{d^4 w_3}{d\xi^4} = 4F\delta(\xi), \quad w_3 < z_0, \quad \xi_2 < \xi < l_2.$$

The solutions to Eq. (7) are given as follows [7]

$$w_1 = A_1 \xi^3 + B_1 \xi^2 + C_1 \xi + D_1,$$

$$w_2 = A_2 \cosh \xi \sin \xi + B_2 \cosh \xi \cos \xi + C_2 \sinh \xi \sin \xi$$

$$+ D_2 \sinh \xi \cos \xi - \frac{F}{2} \sinh |\xi|$$

$$+ \frac{F}{2} \cosh \xi \sin |\xi| + z_0,$$

$$w_3 = A_3 \xi^3 + B_3 \xi^2 + C_3 \xi + D_3. \quad (9)$$

The difficulty of deriving the solutions to Eqs. (7) and (8) is on the particular part. Weitsman's approach [5] of constructing a particular solution for Eq. (7) also applies to Eq. (8). For brevity, the solutions to Eq. (8) are directly given as follows

$$w_1 = a_1 \xi^3 + b_1 \xi^2 + c_1 \xi + d_1,$$

$$w_2 = a_2 \cosh \xi \sin \xi + b_2 \cosh \xi \cos \xi$$

$$+ c_2 \sinh \xi \sin \xi + d_2 \sinh \xi \cos \xi + z_0,$$

$$w_3 = a_3 \xi^3 + b_3 \xi^2 + c_3 \xi + d_3 + 4FH_3(\xi), \quad (10)$$

where A_i , B_i , C_i , D_i and a_i , b_i , c_i , d_i ($i = 1, 2, 3$) in Eqs. (9) and (10) are the unknown constants to be determined. H_3 is a function defined as

$$H_3(\xi) = \int_{-l_1}^{l_2} \int_{-l_1}^{l_2} \int_{-l_1}^{l_2} \int_{-l_1}^{l_2} \delta(\xi) d\xi d\xi d\xi d\xi$$

$$= \begin{cases} 0, & \xi \leq 0, \\ \frac{\xi^3}{6}, & \xi > 0. \end{cases} \quad (11)$$

The matching conditions at $\xi = \xi_1, \xi_2$ can be derived by a variation approach [11] as follows

$$\begin{aligned}
w_1(\xi_1) &= w_2(\xi_1), & \frac{dw_1}{d\xi}(\xi_1) &= \frac{dw_2}{d\xi}(\xi_1), \\
\frac{d^2w_1}{d\xi^2}(\xi_1) &= \frac{d^2w_2}{d\xi^2}(\xi_1), & \frac{d^3w_1}{d\xi^3}(\xi_1) &= \frac{d^3w_2}{d\xi^3}(\xi_1), \\
w_2(\xi_2) &= w_3(\xi_2), & \frac{dw_2}{d\xi}(\xi_2) &= \frac{dw_3}{d\xi}(\xi_2), \\
\frac{d^2w_2}{d\xi^2}(\xi_2) &= \frac{d^2w_3}{d\xi^2}(\xi_2), & \frac{d^3w_2}{d\xi^3}(\xi_2) &= \frac{d^3w_3}{d\xi^3}(\xi_2).
\end{aligned} \quad (12)$$

The above matching conditions in essence indicate the continuity of the displacement, slope, moment and shear force at the separation points of ξ_1 and ξ_2 [2]. The matching conditions are also frequently referred to as the transversality conditions [11, 12].

Two constraint conditions, which indicates the beam displacement at the separation points, are given as follows [7]

$$w_2(\xi_1) = z_0, \quad w_2(\xi_2) = z_0. \quad (13)$$

Here the capillary [13] and the adhesion [14] effects, which play a very important role in the micro/nanostructures, are not considered. Once these effects are considered, the above constraint conditions change correspondingly [14].

For a hinged-hinged beam, the boundary conditions are as follows

$$\begin{aligned}
w_1(-l_1) &= 0, & \frac{d^2w_1}{d\xi^2}(-l_1) &= 0, \\
w_3(l_2) &= 0, & \frac{d^2w_3}{d\xi^2}(l_2) &= 0.
\end{aligned} \quad (14)$$

There are fourteen unknown constants to be determined either for the case of the concentrated load inside contact zone (A_i, B_i, C_i, D_i ($i = 1, 2, 3$), ξ_1 and ξ_2) or for the case of the load outside the contact zone (a_i, b_i, c_i, d_i ($i = 1, 2, 3$), ξ_1 and ξ_2). The transversality, constraint and boundary conditions of Eqs. (12), (13), and (14) give fourteen equations in total to solve the fourteen unknowns. Because of the unknown property of the contact zone (i.e., ξ_1 and ξ_2), solving these fourteen unknowns is a nonlinear problem and the Newton–Raphson method is used [7]. For the Newton–Raphson method to start, the fourteen unknowns need to be guessed first. The computation is not very sensitive to the initial guesses and converges after a few iterations.

3 Results and discussion

As shown in Fig. 1, the concentrated load is at the origin of the coordinate system. In this study the concentrated load starts at the center of the beam and then moves towards the beam right end. When the concentrated load is at the center of a hinged-hinged beam, if the beam is in contact with the substrate, the concentrated load must be inside the contact zone because the loading location is also the location of the maximum beam displacement. If the concentrated load moves rightward and out of the contact zone, the concen-

trated load can only be on the right-side lift-off zone as assumed by Eq. (8). When the concentrated load is inside the contact zone, we have $\xi_1 < 0$ and $\xi_2 > 0$; when the concentrated load is outside the contact zone, we have $\xi_1 < 0$ and $\xi_2 < 0$ for the scenario of the load moving rightward. Therefore, the criterion here to tell whether the concentrated load locates inside or outside the contact zone is $\xi_2 = 0$. Clearly, if F moves leftward, the criterion will be $\xi_1 = 0$.

Here an example with the parameters of $l = 4$, $z_0 = 0.6$ and $F = 0.2$ is presented. Figure 2a shows the variation of total contact length as l_1 increases (or say, F moves rightward) from the center of $l_1 = 2$; Figure 2b shows the variation of the leftside and rightside contact lengths as l_1 increases. When F is inside the contact zone, the rightside contact length is ξ_2 and the leftside contact length is $-\xi_1$; the total contact length here is calculated as $\xi_2 - \xi_1$. As seen in Fig. 2a, when the load moves rightward, the total length increases and then reduces. It needs to point out that the concentrated load at the beam center does not necessarily give the largest total contact length, which is discussed in detail in Ref. [7]. In contrast, the right-side/left-side contact length decreases/increases monotonically as l_1 increases. The rightside contact length of ξ_2 becomes zero when $l_1 \approx 0.692l = 2.768$. F will be outside the contact zone if it moves further rightward. Figure 3 shows the two beam deflection shapes at $l_1 = 0.5l$ and $l_1 = 0.69l$, respectively. Both are the scenario of the concentrated load inside the contact zone. For the symmetric loading of $l_1 = 0.5l$, $-\xi_1 = \xi_2 = 0.6172$; for the asymmetric loading of $l_1 = 0.69l$, $\xi_1 = -1.0798$ and $\xi_2 = 0.000303$.

When $l_1 > 0.692l$, the concentrated load is outside the contact zone; Equation (7) becomes invalid and Eq. (8) applies. Figure 4 shows the two cases of F outside the contact zone with $l_1 = 0.7l$ and $l_1 = 0.75l$, respectively. In Fig. 4a of $l_1 = 0.7l$, $\xi_1 = -1.105$ and $\xi_2 = -0.04778$; In Fig. 4b of $l_1 = 0.75l$, $\xi_1 = -1.225$, and $\xi_2 = -0.276$. The l_1 difference between Fig. 3b and Fig. 4a is small and it is found that their differences in the beam deflection shapes and contact lengths are also small. The beam is an Euler–Bernoulli beam and the

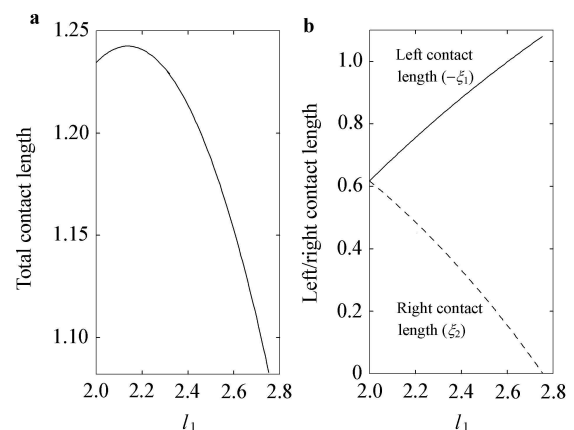


Fig. 2 **a** The total contact length versus l_1 ; **b** The leftside/rightside contact length versus l_1

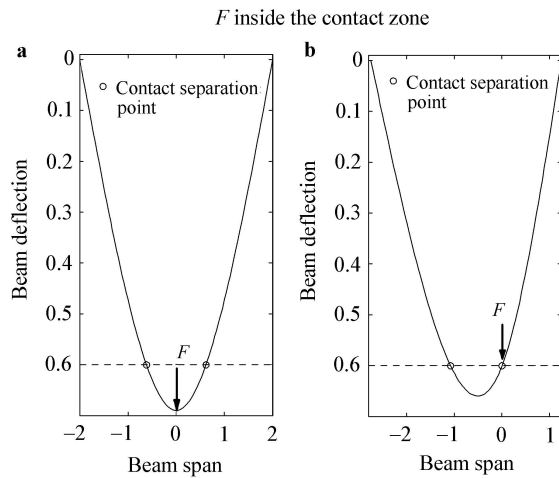


Fig. 3 Beam deflection shapes with the concentrated load inside the contact zone. **a** $l_1 = 0.50l$; **b** $l_1 = 0.69l$

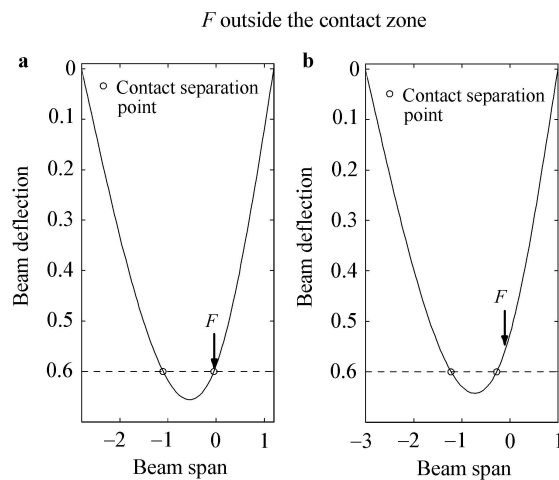


Fig. 4 Beam deflection shapes with the concentrated load outside the contact zone. **a** $l_1 = 0.70l$; **b** $l_1 = 0.75l$

foundation is a linear Winkler foundation. The nonlinearity of the tensionless contact is caused by the unknown feature of the contact zone. Mathematically, the fact that the concentrated load moves out of the contact zone corresponds to the switching of the governing equations from Eq. (7) to Eq. (8), which introduces another nonlinearity and this nonlinearity does not cause any abrupt change.

4 Summary

An asymmetric concentrated load can be either inside or outside the contact zone of a flexural beam with a nonzero gap distance. Two sets of governing equations are needed for these two scenarios. A criterion is established to tell whether the concentrated load is inside or outside the contact zone. As the concentrated load moves out of the contact zone, the changes of both the beam deflection shape and the contact length are shown to be smooth.

References

- 1 Zhang, Y.: Extracting nanobelt mechanical properties from nanoindentation. *J. Appl. Phys.* **107**, 123518 (2010)
- 2 Zhang, Y., Zhao Y.P.: Modeling nanowire indentation test with adhesion effect. *J. Appl. Mech.* **78**, 011007 (2011)
- 3 Mastrangelo, C.H., Hsu, C.H.: Mechanical stability and adhesion of microstructures under capillary forces - part I: Basic theory. *J. Microelectromech. Syst.* **2**, 33–43 (1993)
- 4 Jones, E.E., Begley, M.R., Murphy, K.D.: Adhesion of micro-cantilever subjected to mechanical point loading: Modeling and experiments. *J. Mech. Phys. Solids* **51**, 1601–1622 (2003)
- 5 Weitsman, Y.: On Foundations that reacts in compression only. *J. Appl. Mech.* **37**, 1019–1030 (1970)
- 6 Weitsman, Y.: A tensionless contact between a beam and an elastic half-space. *Int. J. Engr. Sci.* **10**, 73–81 (1972)
- 7 Zhang, Y., Murphy, K.D.: Response of a finite beam in contact with a tensionless foundation under symmetric and asymmetric loading. *Int. J. Solids Struct.* **41**, 6745–6758 (2004)
- 8 Zhang, Y., Murphy, K.D.: Tensionless contact of a finite circular plate. *Acta Mech. Sin.* **28**, 1374–1381 (2012)
- 9 Biot, M.A.: Bending of an infinite beam on an elastic foundation. *J. Appl. Mech.* **4**, 1–7 (1937)
- 10 Castillo, J., Barber, J.S.: Lateral contact of slender prismatic bodies. *Proc. R. Soc. London, Ser. A* **453**, 2397–2412 (1997)
- 11 Kerr, A.D.: On the derivation of well posed boundary value problems in structural mechanics. *Int. J. Solids Struct.* **12**, 1–11 (1976)
- 12 Liu, J.L.: Theoretical analysis on capillary adhesion of micro-sized plates with a substrate. *Acta Mech. Sin.* **26**, 217–223 (2010)
- 13 Liu, J.L., Feng, X.Q.: On elastocapillarity: A review. *Acta Mech. Sin.* **28**, 928–940 (2012)
- 14 Zhang, Y., Zhao, Y.P.: Flexural contact in MEMS stiction. *Int. J. Solids Struct.* **49**, 2203–2214 (2012)